Electronic Supplementary Material (ESI) for Nanoscale Advances.
This journal is © The Royal Society of Chemistry 2022

Supplementary Information : A van der Waals Heterojunction Based on Monolayers of MoS_2 and WSe_2 for Overall Water Splitting

Paul Dalla Valle* and Nicolas Cavassilas

Aix Marseille Université, CNRS, Université de Toulon, IM2NP UMR 7334, 13397, Marseille, France

E-mail: paul.dalla-valle@im2np.fr

Contents

1 Supplementary 1. Calculations of the TMDC absorbance

In our model, we consider the absorption enhancement system as simple devices which increase the number of passages of light in the active core as presented in Figure 1. We refer this number of passages as N in the main text.

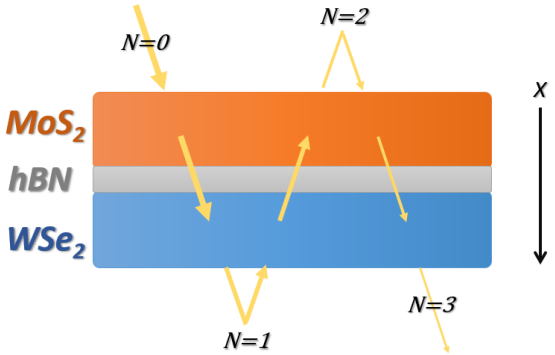

Figure 1: Representation of the model used to simulate absorption enhancement system. Due to its large gap, hBN does not absorb photon.

We analytically calculate the absorption in MoS_2 and WSe_2 (respectively A_M and A_W) according to this parameter N and the energy E of the photon:

$$A_M(E,N) = (1-e^{-\alpha_M L_M}) + e^{-\alpha_M L_M} e^{-2\alpha_W L_W}(1-e^{-2\alpha_M L_M}) \frac{1-e^{-(N-1)(\alpha_M L_M+\alpha_W L_W)}}{1-e^{-(\alpha_M L_M+\alpha_W L_W)}} \quad (1)$$

$$A'_W(E,N) = e^{-\alpha_M L_M}(1-e^{-2\alpha_W L_W}) \frac{1-e^{-(N-1)(\alpha_M L_M+\alpha_W L_W)}}{1-e^{-(\alpha_M L_M+\alpha_W L_W)}} \quad (2)$$

$$A_W(E,N) = A'_W(E,N) + (1-A_M(E,N)-A'_W(E,N))(1-e^{-\alpha_W L_W}) \quad (3)$$

where α_M and α_W are the absorption coefficients of MoS_2 and WSe_2 respectively, L_M and L_W are the thicknesses of MoS_2 and WSe_2 respectively. A'_{WSe_2} is the absorption in WSe_2 for $N-1$ passages (*i.e.* without taking into account the last passage).

2 Supplementary 2. Discussion about the external radiative efficiencies in isolated TMDC and their heterojunction

In our model, we assumed that the external radiative efficiencies of the heterojunction (ERE_{HJ}) and isolated materials (ERE_{TMDC}) were equal. This assumption comes from the fact that, for a fixed ERE_{TMDC}, we cannot determine ERE_{HJ}. We then chose the latter as being the least favourable for the efficiency of the system so that we do not overestimate the photoelectrochemical efficiency. Figure 2 shows the photoelectrochemical efficiency versus ERE_{HJ}. The ERE_{TMDC} being set to 10^{-1}, we thus see that the worst case occurs when $ERE_{HJ} = ERE_{TMDC}$. This case, considered in the main text, limits the recombination in the heterojunction, increases the voltage drop induced by the recombination and then reduces the efficiency of the system. Reducing the ERE_{HJ} enables to reduce the region without hBN, which is not useful for the water splitting.

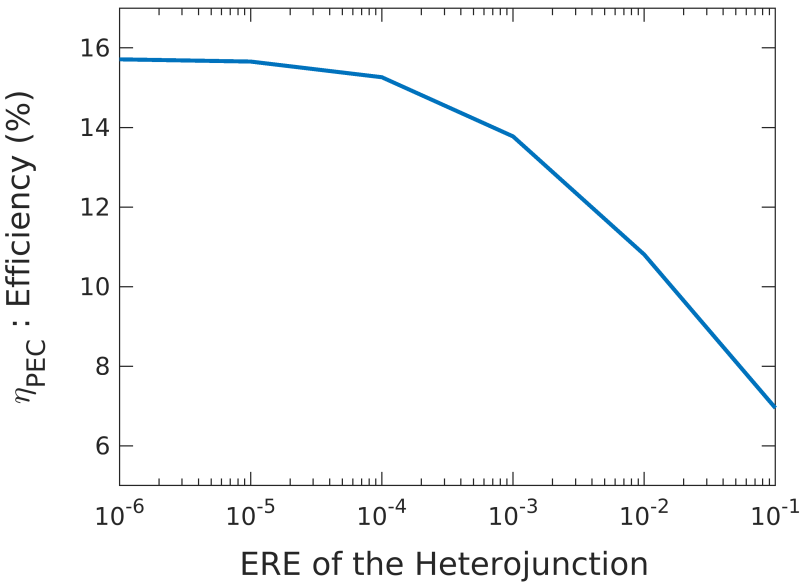

Figure 2: Photoelectrochemical efficiency versus the external radiative efficiency of the heterojunction, ERE_{TMDC} is set to 10^{-1} all other parameters being fixed.

Practically, we expect the ERE_{HJ} to be lower than the ERE_{TMDC} because of the defects induced during the heterojunction fabrication.

3 Supplementary 3. Computational methods of the *ab initio* calculations

We used *ab initio* calculations to study the band structures and absorption coefficients of 2D MoS_2 and WSe_2 (isolated and in heterojunction). These calculations were developed in the framework of plane-wave density functional theory implemented in the Quantum ESPRESSO[1 2] package. The van der Waals interaction is described with the functional rVV10[3] which gives the most accurate results for intralayer and interlayer lattice constants for 28 layered materials which have been experimentally confirmed.[4] The electron-ion interaction is described with pseudopotentials produced using the code ONCVPSP (Optimized Norm-Conserving Vanderbilt PSeudoPotentials)[5] from pseudo-dojo.org.[6] The energy cutoff in the calculations was set to be 1000 eV, and the total energy was converged to better than 10^{-6} eV.

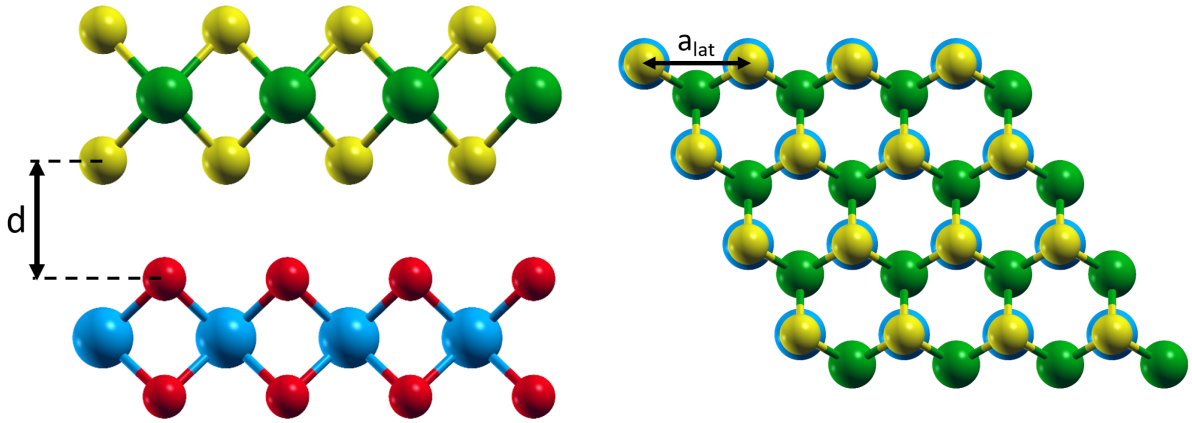

Figure 3: Side (a) and top (b) views of the MoS_2/WSe_2 heterojunction. The Mo, S, W and Se atoms are represented by blue, red, green and yellow spheres, respectively. a_{lat} is the relaxed lattice parameter of heterojunction and d is the interlayer distance between the TMDC monolayers, taking the van der Waals interactions into account.

The MoS_2/WSe_2 heterojunction was formed with the stacking configuration depicted in Figure 3 which is the most stable configuration.[7] The mesh parameter a_{lat} is calculated

in order to minimise the total energy of the system. We then find a_{lat} = 3.28 Å. The distance d of 3.15 Å between the two monolayers is calculated by taking into account the van der Waals interactions. Each slab is separated with a vacuum layer larger than 20 Å along the z-direction (*i.e.* perpendicular to the slabs) to prevent unwanted interactions. The Hellmann-Feynman forces were converged to less than 25 meV/Å to obtain the relaxed structures. The 2D Brillouin-Zone is sampled with a (12x12x1) Monkhorste-Park mesh.

To calculate the absorption coefficient of the materials, we used the post-processing code epsilon.x from Quantum ESPRESSO. This code provides the real and imaginary part of the dielectric tensor from DFT eigenvalues and eigenvectors.

4 Supplementary 4. Band structures of the isolated TMDC

The band structures of the isolated TMDCs are calculated with DFT and are presented in Figure 4. The lattice parameters of the monolayers are calculated after relaxation and are equal to 3.215 and 3.345 Å for MoS_2 and WSe_2 respectively.

MoS_2 and WSe_2 are both direct band gap semiconductors and their energy band gaps are equal to 1.65 and 1.55 eV respectively.

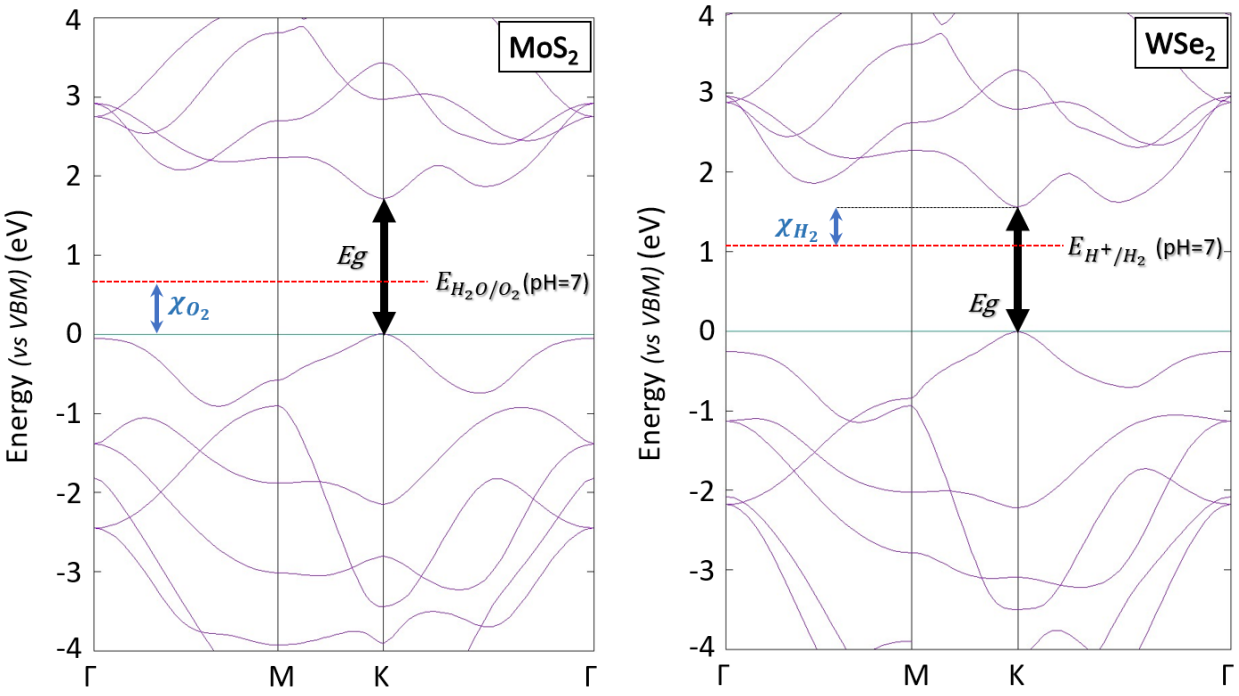

Figure 4: Band structure of an isolated monolayer of MoS_2 (a) and WSe_2 (b) from DFT. E_{H_2O/O_2} and E_{H^+/H_2} are the standard potential of oxidation (H_2O/O_2) and reduction (H^+/H_2) respectively. χ_{O_2} (χ_{H_2}) is the potential difference between the VBM (CBM) of MoS_2 (WSe_2) and E_{H_2O/O_2} (E_{H^+/H_2}).

5 Supplementary 5. Extrapolation of the parameter N

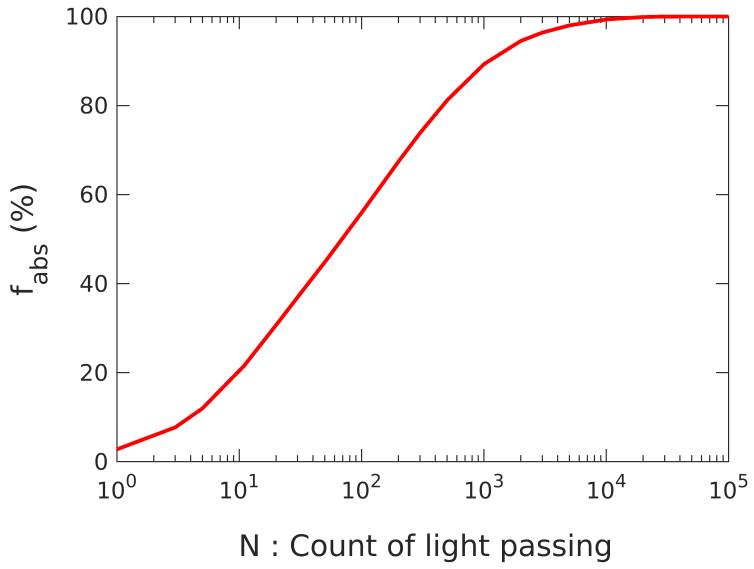

Figure 5: Representation of the fraction of incident light absorbed by the TMDCs versus N. Only photons with energy higher than the band gap are considered.

Although the parameter N is not representative of the operation of an optical enhancement system, it enables to calculate, over an energy range $[E_1, E_2]$, the fraction of incident light that must be absorbed by the TMDC versus N. We express this fraction, denoted by f_{abs}, with the expression:

$$f_{abs}(N) = \frac{N_{ph}^{abs}(N)}{N_{ph}^{in}} \times 100 \tag{4}$$

where N_{ph}^{abs} is the photons flux absorbed by the active core (*ie* MoS_2 or WSe_2) and N_{ph}^{in} is the incident photon flux on the energy range considered, given by

$$N_{ph}^{in} = \frac{1}{q}\int_{E_1}^{E_2} \frac{AM1.5G(E)}{E} \mathrm{d}E \tag{5}$$

$$N_{ph}^{abs}(N) = \frac{1}{q}\int_{E_1}^{E_2} \frac{AM1.5G(E)}{E} A(E,N) \mathrm{d}E \tag{6}$$

$A(E,N)$ is the total absorbance :

$$A(E,N) = A_M(E,N) + A_W(E,N) \tag{7}$$

with $A_M(E,N)$ and $A_W(E,N)$ are the absorbance of MoS_2 and WSe_2 respectively, as defined in eq (1).

Here, we are interested in energies higher than the band gap ($E_1 = Eg$ and $E_2 = +\infty$)and we plot f_{abs} versus N (Figure 5). To get an efficiency of 10% with high-performance materials, we need $N = 99$. This corresponds to an absorption of 56% of the incident light in this energy range.

A more detailed analysis of the absorbance $A(E,N)$ versus N shows that, to maximise the efficiency, we must design the absorption enhancement system to increase the absorption of the photons close to the band gap energy. Figure 6 shows the total absorbance $A(E,N)$ versus the energy E for different values of N.

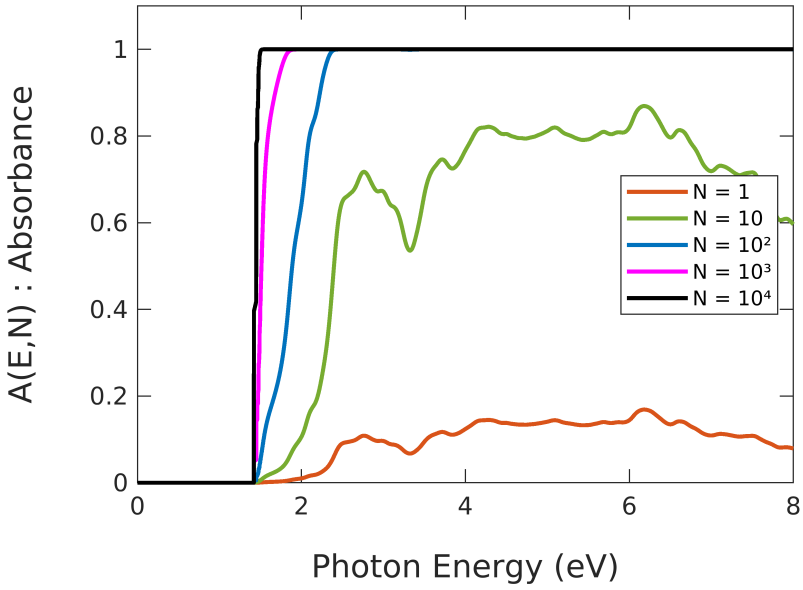

Figure 6: Plot of the total absorbance in the TMDCs versus the energy E for different values of N

6 Supplementary 6. Influence of radiative efficiency on the J (V) characteristics of TMDC

To understand the influence of the external radiative efficiency (ERE) on the TMDCs, we present, in Figure 7, the current-voltage characteristic of MoS_2 for different ERE. Increasing the external radiative efficiency increases the open-circuit voltage of the TMDC. This voltage is of capital importance for our system since the voltages generated by the TMDCs must be large enough to compensate for the losses and reach the electrochemical reaction potential.

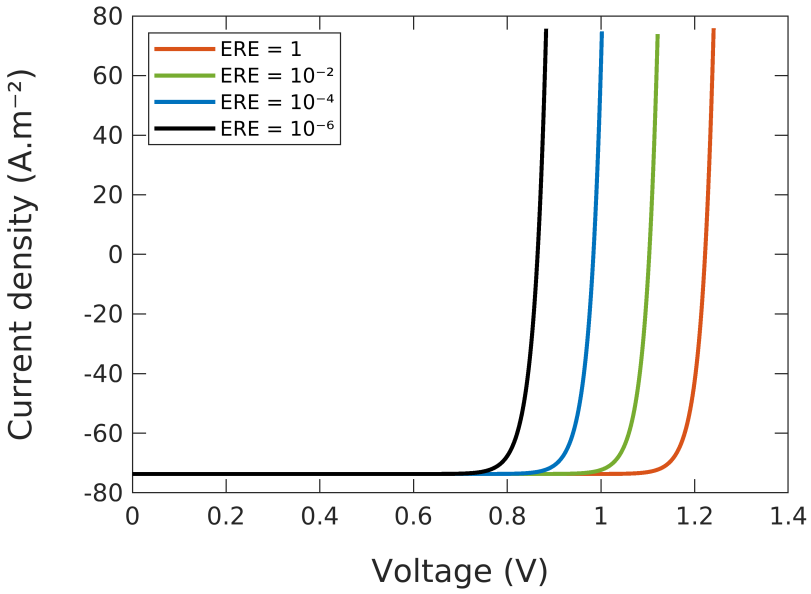

Figure 7: Current-voltage characteristics of MoS_2 for different external radiative efficiency ERE

7 Supplementary 7. Influence of the exchange current density on the catalysis overpotentials

To highlight the importance of the catalytic exchange current density $J_{0,a/c}$ on the behaviour of the system, we present, in Figure 8, the electrochemical overpotential versus the current density for several $J_{0,a/c}$ (using Butler Volmer's kinetics with the hypothesis $\alpha_a = \alpha_c = 0.5$).[8] We show that for a given current density, increasing the exchange current density, reduces the overpotential. Thus, for a current density of 1 mA.cm^{-2}, a $J_{0,a/c}$ of 10^{-7} mA.cm^{-2} generates an overpotential of 420 mV. This overpotential drops to 180 mV for a $J_{0,a/c}$ of 10^{-3} mA.cm^{-2}.

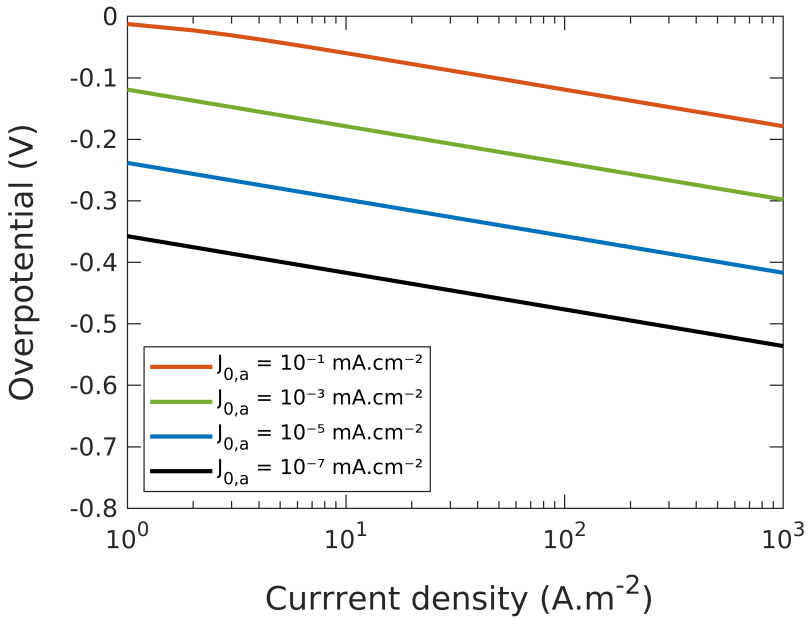

Figure 8: Butler-Volmer kinetics for different exchange current densities. The overpotential is negative since it corresponds to a loss for our device.

References

(1) Giannozzi, P. et al. QUANTUM ESPRESSO: A Modular and Open-Source Software Project for Quantum Simulations of Materials. *Journal of Physics: Condensed Matter* **2009**, *21*, 395502.

(2) Giannozzi, P. et al. Advanced Capabilities for Materials Modelling with Quantum ESPRESSO. *Journal of Physics: Condensed Matter* **2017**, *29*, 465901.

(3) Sabatini, R.; Gorni, T.; de Gironcoli, S. Nonlocal van Der Waals Density Functional Made Simple and Efficient. *Physical Review B* **2013**, *87*, 041108.

(4) Björkman, T.; Gulans, A.; Krasheninnikov, A. V.; Nieminen, R. M. Van Der Waals Bonding in Layered Compounds from Advanced Density-Functional First-Principles Calculations. *Physical Review Letters* **2012**, *108*, 235502.

(5) Hamann, D. R. Optimized Norm-Conserving Vanderbilt Pseudopotentials. *Physical Review B* **2013**, *88*, 085117.

(6) van Setten, M. J.; Giantomassi, M.; Bousquet, E.; Verstraete, M. J.; Hamann, D. R.; Gonze, X.; Rignanese, G. M. The PseudoDojo: Training and Grading a 85 Element Optimized Norm-Conserving Pseudopotential Table. *Computer Physics Communications* **2018**, *226*, 39–54.

(7) Li, W.; Wang, T.; Dai, X.; Wang, X.; Zhai, C.; Ma, Y.; Chang, S.; Tang, Y. Electric Field Modulation of the Band Structure in MoS2/WS2 van Der Waals Heterostructure. *Solid State Communications* **2017**, *250*, 9–13.

(8) Fountaine, K. T.; Lewerenz, H. J.; Atwater, H. A. Interplay of Light Transmission and Catalytic Exchange Current in Photoelectrochemical Systems. *Applied Physics Letters* **2014**, *105*, 173901.